**I J C T A**, 9(16), 2016, pp. 8061-8070


# Hybrid Energy Storage Devices based TET system design for Powering the ICP Devices

**R. Narayanamoorthi*, A. Vimala Juliet*, A. Dominic Savio* and Pradeep Vishnuram***

**ABSTRACT**

This paper aims to develop a system used for transferring the transcutaneous electric power by means of an inductive power transfer to power the intracranial pressure (ICP) measurement sensor for a lifetime. Class-E power oscillator is used in the Primary side of the system along with a feedback network containing crystal to compensate operational frequency changes. The implanted section consists of spiral coupled coils and a rectifier circuit maintaining the output voltage as constant. A rechargeable battery is complemented by an energy storage element of electric double-layer capacitor to form a hybrid energy storage system. The designed system aims at transferring 105 mW and outut voltage of 3V with the frequency of 13.56 MHz and the simulation results shows that the super capacitor takes only 2.8 seconds to charge up for 1-minute operation of ICP for quick data collection, while longer durations of monitoring can be supported by the battery.

***Key Words:*** Class E amplifier, Battery, ICP, super capacitor, wireless power.

## 1. INTRODUCTION

The intracranial pressure (ICP) is increased in the 4 ventricles (cavities) of the brain, connected by narrow pathways due to the presence of cerebrospinal fluid. It is commonly called as "water on the brain" or Hydrocephalus. Because of these the ventricular shunt block frequently and their failure is hard to sense, consuming much clinical time and computed tomography or magnetic resonance imaging [2]. But if the ICP is measured regularly the shunt failure is easy to detect [3]. Water on the brain is a lifetime disorder and the monitoring system needs to be fully implanted without wires to evade the infection risk. The measured data needs to be transmitted outside the brain for the analysis at the sampling rate of around 100Hz and it requires the battery power of 10mW, which renders a battery unable to provide lifetime operation, and to be of a size sufficiently small to implant [4]. Changing a rechargeable battery needs operation and leads risk of new infection, therefore the best alternative solution is wireless power transfer technologies. An inductive power transfer (IPT) system, as shown in Fig. 1, can be used to enable the power transfer across the skin without direct electrical contacts, although power losses and resultant heating effect need to be managed properly to avoid tissue damage [3]. An inductive power transfer (IPT) system, as shown in Fig. 1, can be used to enable the power transfer across the skin without direct electrical contacts, although power losses and resultant heating effect need to be managed properly to avoid tissue damage [3]. Heat dissipation around implanted components while delivering large amount of power (15 W) has been reported in sheep studies [4] and a temperature rise can be less than 2°C.

The IPT power supply can be used to charge an internal battery to keep the ICP device functioning when the primary external device is not available. However, there are two main drawbacks with rechargeable batteries for this application: 1) slow charging time and 2) limited charging cycles. Both of these limitations

* Faculty of Engineering and Technology, SRM University, Kattankulathur-603203, Chennai, India, *Email: narayanamoorthi.r@gmail.com*

can be mitigated by including super capacitors. Fast charging capability of a super capacitor allows quick real-time monitoring of a patient when needed.

Although ICP device concept is relatively easy to understand, feasible and practical design of such a system is a complex task. The natural size constrains and the intricate human body environment presents numerous technical challenges. The required miniaturized design, the poor availability of respective miniaturized components to produce marketable systems , the low signal-to-noise ratio presented by internal signal interferences and biofouling effects [9. A combination of rechargeable battery and super capacitors can provide near instant device power needs and support a lifetime operation. The use of super capacitors as energy storage devices is well known and it is a subject of ongoing research.

## 2. SYSTEM OVERVIEW

The proposed system can be split into two sections of outside the body unit(primary) and inside the body unit(secondary), as shown in Fig. 2. The primary consists of a class E amplifier. It produces high frequency ac currents in the transmitter coil, which generates an alternating magnetic field. The resonant circuit is tuned to the operating frequency to increase the power transferred. The secondary unit consists of a receiver coil, resonant circuit, rectifier, energy storage elements, processing unit, and a load. The load consists of ICP monitoring device, the pressure sensor, data acquisition electronics, and microprocessor. The receiver coil loosely couples with the magnetic field from the primary and is tuned with a capacitor to the operating frequency. The capacitor forms a resonant tank with the inductance of the receiver coil, maximizing the power transferred.

A super capacitor and a lithium-ion polymer battery are used to deliver power to the load (ICP monitor) for both short-term and long-term operations. These two operating modes are determined based on duration of time the primary coil is applied to the head, as shown in Fig. 3. Although it is possible to transfer the power across a larger distance between the primary and implanted devices, to reduce the coil size and power losses, the actual distance we experimented on was set at about 10 mm, sufficient to transfer power across the skin.

## 3. WIRELESS POWER TRANSFER CIRCUITS

To provide the power source for the hybrid energy storage system an IPT system has been constructed. Fig. 4 shows the physical configuration of the primary circuit and secondary circuit of the system shown in Fig.

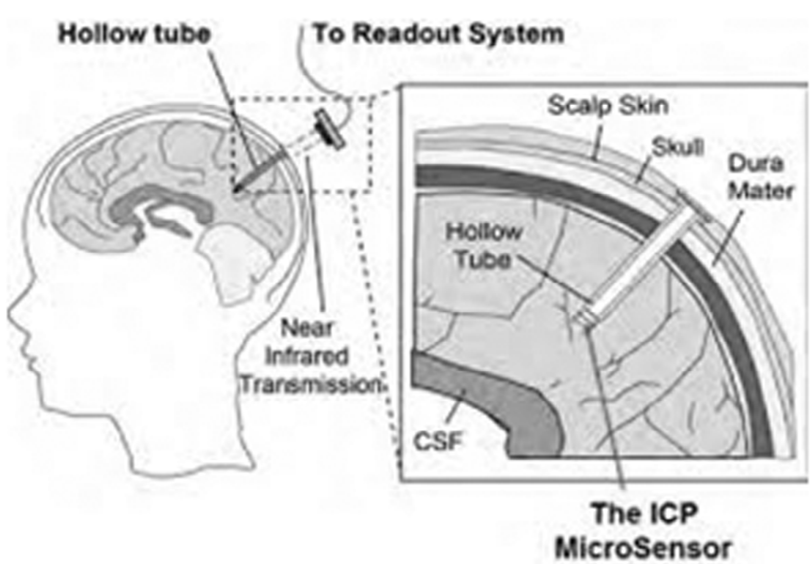


**Figure 1: Fully implanted ICP monitor powered by IPT [3]**

2. To analyze the performance of the hybrid energy storage system, the separation between the two inductor coils was kept at 10 mm—this is representative of the separation that might occur across the skull. The operating frequency of the system is chosen as 13.56MHz. This frequency is within the wireless power consortium Qi standard frequency range, and offers a good balance between the output power transfer capacity, power losses, and the system size [10]– [12].

### 3.1. Primary Side Power Converter

For the ICP system design, power consumption and miniaturization are critical aspects. Space constrains highly limit transmitter coil size, requiring higher operating frequencies, which leads to much increase in the abortion of electromagnetic (EM) energy by dissipative medium, like biological tissue. A robust power inverter is then needed to efficiently supply enough power to the transmitter coil. Since Class-E transistor tuned power amplifiers offers higher power efficiency at higher transmission frequencies when compared with others, like Class-B and C amplifier, it's largely used in medical application to inductively power up implantable devices. It is giving high coil voltages without a high supply voltage.

The Class-E output circuit is a multi vibrator load network. The switch Q is operated by a clock like high frequency signal. When the switch is 'on', the oscillation is due to the series resonant $L_2$–$C_2$ tank. When the switch is 'off', the oscillation comes from the $C_1$–$C_2$–$L_2$ tank. At the same time a DC current from $V_{cc}$ through the choke coil $L_{choke}$ is charging $C_1$. Proper component selection can make the switch voltage and its slope both zero at turn 'on' state, the voltage–current product low during the entire operation cycle [12]. This working condition is established by attending the following six criteria:

- During switch 'on' state, the transistor behaves as a low resistance closed switch.
- During switch 'off' state, the transistor behaves as an open switch.
- The voltage across the transistor is allowed to rise only after the transistor stopped to conduct current through its terminals, avoiding high power losses during switching transitions.
- The current through the transistor is allowed to rise only after the transistor stopped to sustain voltage across its terminals, avoiding high power losses during switching transitions.
- Zero voltage across the transistor just before the switch reaches the 'on' state, to avoid losing the energy stored at the shunt capacitor $C_1$ (the shunt capacitor is the total capacitance comprised by the parallel capacitance and the transistor's parasite capacitance).

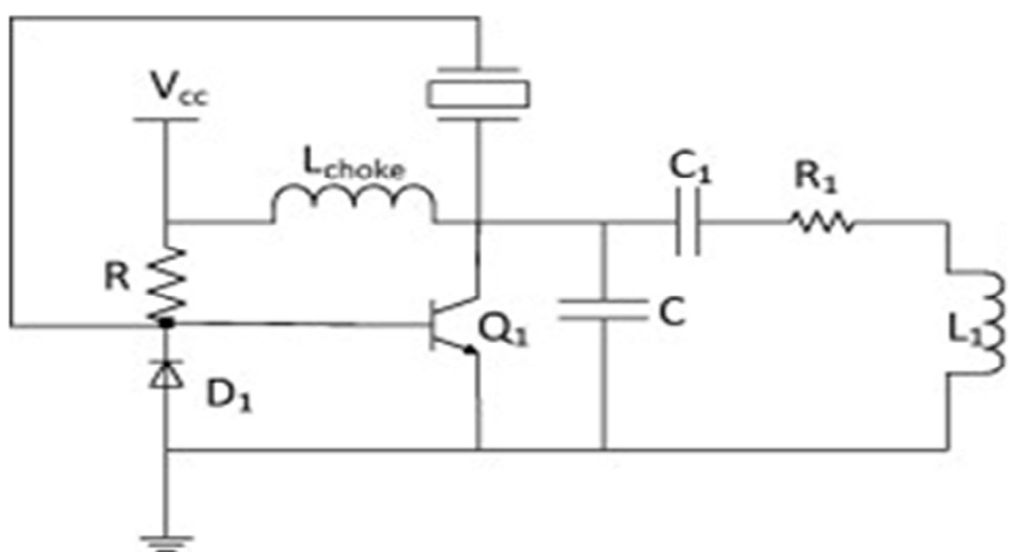


**Figure 2: simplified schematic of a low-order Class-E amplifier.**

- Zero voltage slope just before switch reaches the 'on' state, avoiding high power dissipation through the transistor during transition to 'on' state.

The desired transistor's voltage and current waveforms are shown in Fig. 4. Basically, during switch 'on' state, the transistor behaves as a low resistance closed switch. During switch 'off' state, the transistor behaves as an open switch. The rise time of the transistor voltage is delayed until after the current has reduced to zero and it returns to zero, with slope nominally zero, before the current through it begins to rise. This timing response is accomplished by means of a multivibrator load network.

### 3.2. Secondary circuit

To maximize the power at the secondary, a tuning capacitor is added to compensate for the inductance of the secondary coil. The inductor and tuning capacitor resonate approximately at the operating frequency É. The compensation circuit was chosen to be parallelly tuned as this circuitry acts as a current-source at the full resonance. For the intended charging applications for a super capacitor and a battery, the current-source is more appropriate in this research. The current-source of the parallel-tuned circuit would be equal to the short circuit current $I_{sc}$ of the secondary coil. At the separation distance of 1 cm between the primary and secondary coils, $V_{oc(rms)}$ and $I_{sc(rms)}$ were measured to be 3.6 V and 0.8 A, respectively. A capacitance of 250 nF was connected in parallel with the secondary coil.

A rectifier is needed to convert the ac source from the pickup resonant circuit to dc to drive the load. A push–pull current doubler synchronous rectifier with two low side MOSFETS has proved to have lower power losses than a full bridge rectifier [14]. Interestingly, the circuit operation of such a push–pull synchronous rectifier is the inverse of the primary push–pull resonant converter, which requires complicated switch drive circuitry to achieve ZVS. At a low current level, the two MOSFETS of current doubler can be replaced with two low side Schottky diodes, as shown in Fig. 3, without introducing significant power losses [15]. The current doubler configuration also has the advantage of doubling the output dc charging current.

## 4. SIMULATION RESULTS

The model was simulated with the two features. 3D plots were generated for the electric potential and the magnetic flux density, as given in Fig. 4 and Fig. 5. The figures demonstrate how the electric potential and magnetic flux density is maximum around the primary coil

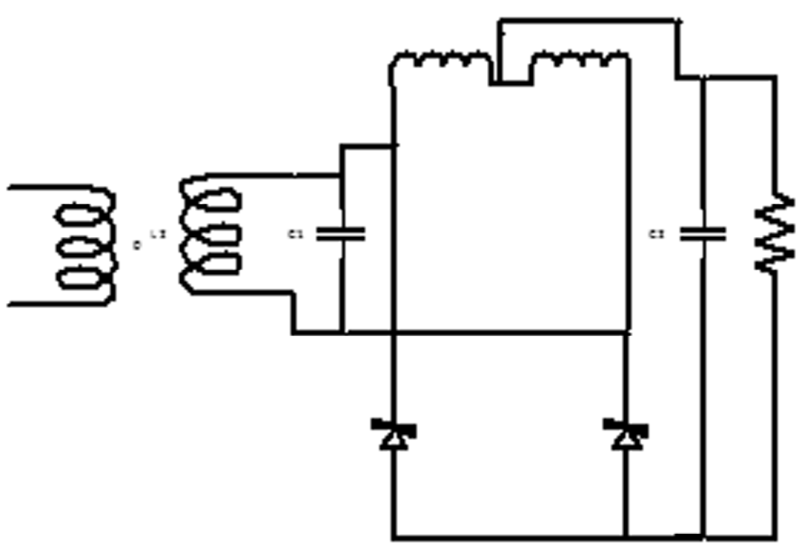

**Figure 3: Current doubler rectifier circuit.**

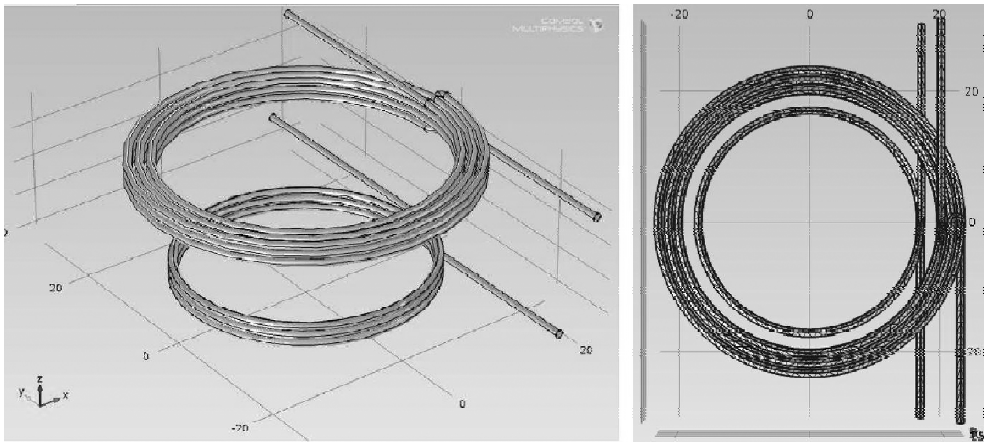

**Figure 4: 3D coil setup in COMSOL and coarse triangular mesh.**

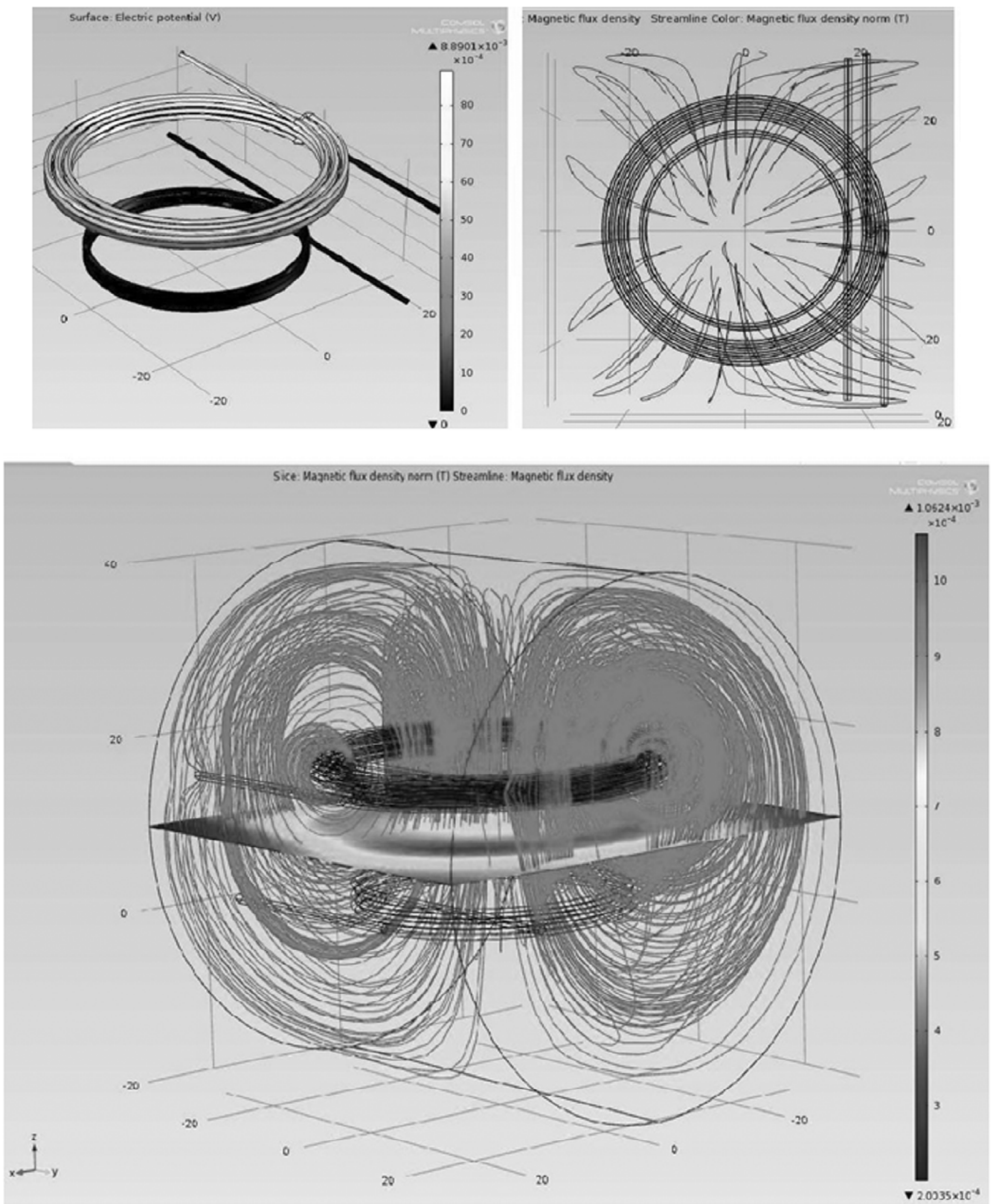


**Figure 5: Electric potential and magnetic flux density**

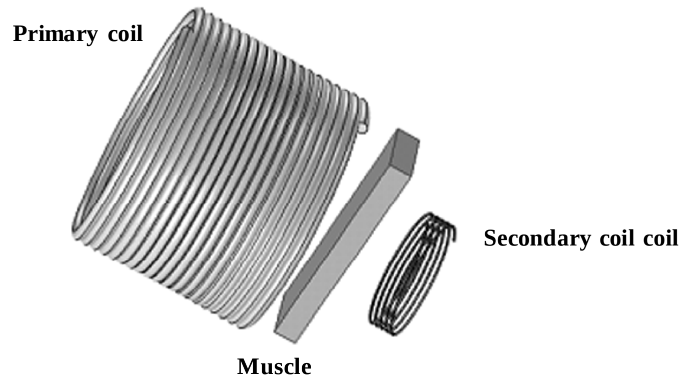


**Figure 6: COMSOL Design of implanted coil setup.**

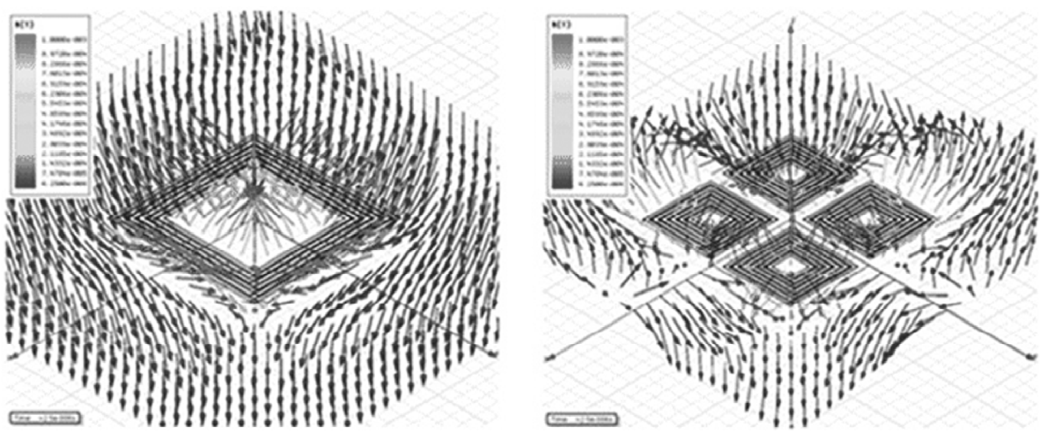

**Figure 7: Magnetic field distribution**

The electric potential is highest at the excited terminal and gradually decreases along the perimeter of the two coils. The magnetic flux linkage between the two coils is also evident from the figure. The transcutaneous Energy System has been designed to supply a power of 100 mW and output a 3.3 V stable DC voltage $V_{out}$, resulting in a system load $R_{load}$ of 108.9. 13.56MHz is chooses as the inductive link frequency. The secondary coil outer radius has been fixed at 5.5 mm and the inner radius fixed at 2.5 mm. Based on 29 turns of 44 AWG Litz wire the self-inductance of $L_2$ is evaluated around 8.0lH. The primary coil outer radius has been calculated and the inner radius has been fixed at 11 mm. The self-inductance of $L_1$, based on 41 turns of 44 AWG Litz wire, is approximately 70.7lH. The resulting coil specifica-tions are summarized and presented in Table 1.

For this set of coils yields a maximum efficiency of 49.6% and overall gain of 0.76. The link specifications for this setup are listed in Table 1, along with the simulation results, performed with electronics workbench MULTISIM.

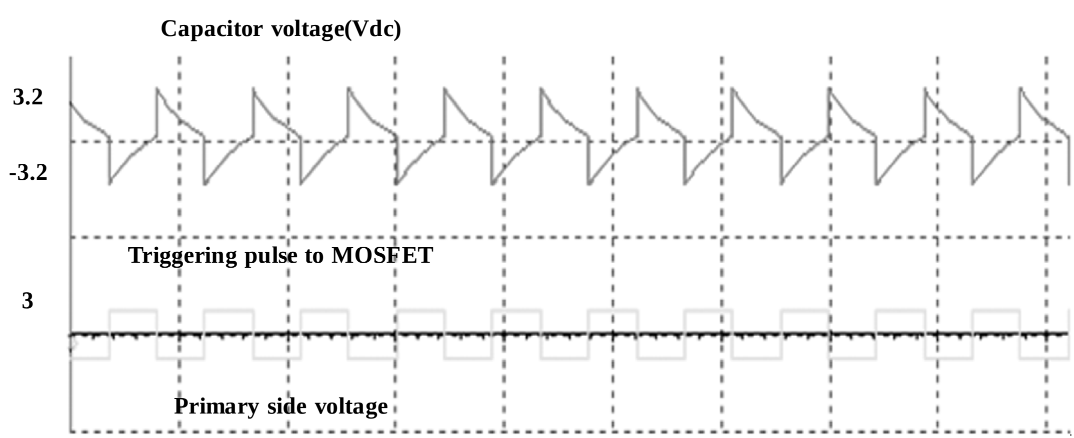

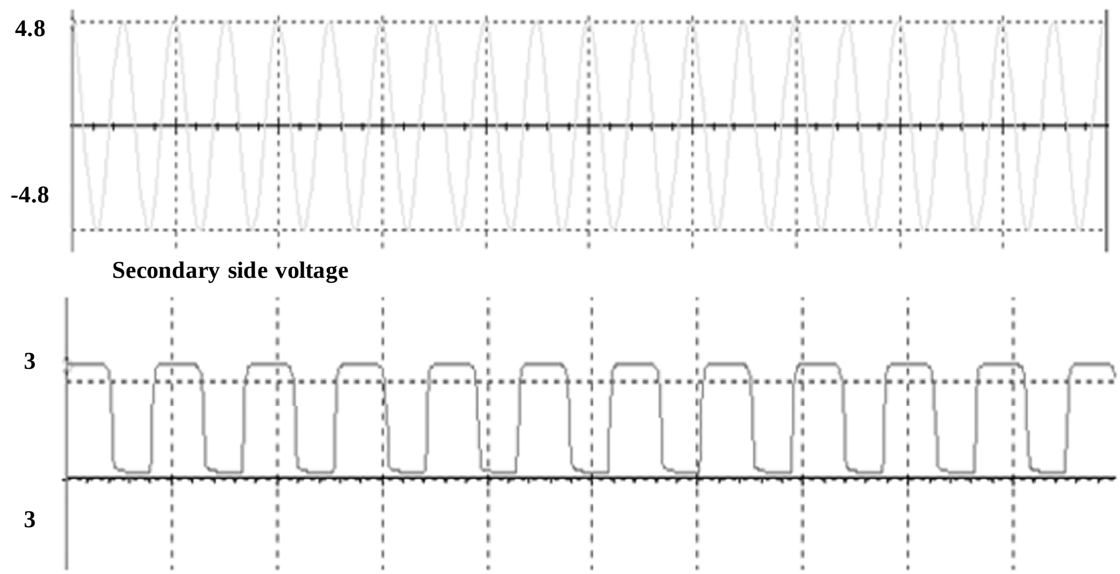


**Figure 8: Simulated results of the proposed circuit**

**Table 1**
**Specification and Results of the simulation**

| | *Theoretical values* | *Simulation* | *Units* |
|---|---|---|---|
| Freq. | 1 | 1 | MHz |
| Duty cycle | 50 | 50 | % |
| $C_p$ | 249 | 270 | pF |
| $C_s$ | 3.02 | 3.30 | nF |
| $L_{choke}$ | 1.5 | 1.5 | mH |
| $C_2$ | 2.19 | 2.20 | nF |
| $V_{CC}$ | 5 | 5 | V |
| $Pi_n$ | 202 | 240 | mW |
| $P_{out}$ | 100 | 105 | mW |
| $V_{out}$ | 3.30 | 3.30 | V |
| $G_{link}$ | 49.6 | 43.8 | % |

The simulation results show that an efficiency of 43.8% at an inter-coil distance of 75 mm is achieved, which is in good agreement with the theoretical value. The difference may arise from underestimation of component losses. The proof-of-concept prototype, built to validate the design, had an efficiency of 21.0%. It successfully delivered a cur-rent of 27 mA and a stable 3 V DC output voltage to a load of 110 X. The mismatching between the theoretical efficiency (49.6%) and the measured results may be due to super estimation of the Q factors and coupling coefficient.

## 5. EXPERIMENTAL VERIFICATION

A prototype wireless power supply circuitry with two com-bined energy storage devices was built, as shown in Fig. 9. The size of the proof-of-concept receiver is 93 mm × 83 mm; how-ever, the use of the standard surface mount technology could render this circuit sufficiently small for implantation. The prototype supplied 32-mW continuous power to the load, and the performance of the system was tested with the short-term and long-term operation modes. The short-term performance was assessed utilizing the supercapacitor as the storage device to power the load. The long-term performance was assessed with the battery charged for a long duration of time and then discharged until reaching the minimum voltage allowed.

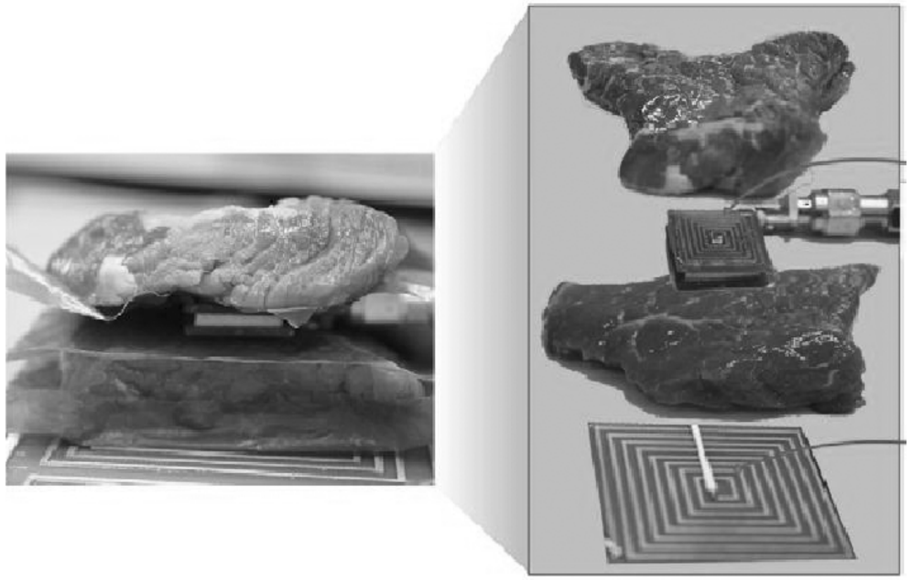

**Figure 9: Experimental Setup**

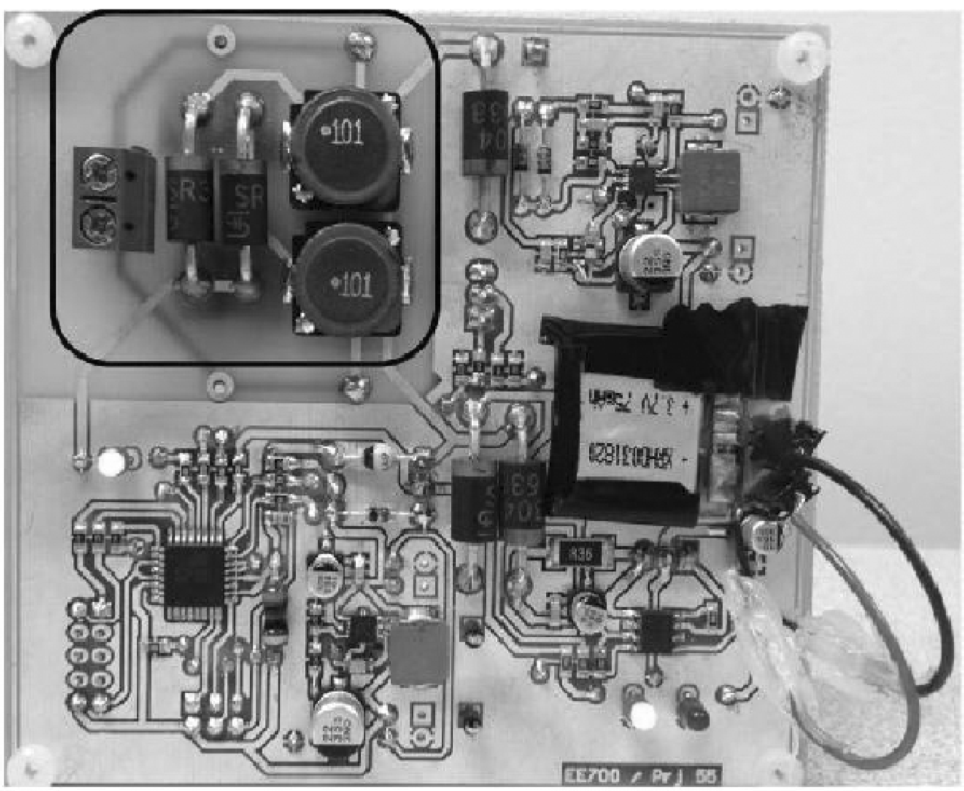

**Figure 10: Powering circuit**

The charging and discharging profile of the supercapacitor takes approximately 3 s for the superca-pacitor to charge up to its rated voltage of 5.5 V. The voltage across the supercapacitor was then regulated at 5.5 V using a shunt switch to ensure that it does not exceed the maximum supercapacitor voltage, preventing it from damage. Once the charging of the supercapacitor was finished, the primary coil was removed from the secondary. The supercapacitor, then, supplied power to the load and it took ~ 60 s to discharge from 5.5 to 1.7 V. The voltage across the supercapacitor is not fully discharged to 0 V, as the buck–boost circuitry has an under voltage lockout threshold of ~ 1.7 V. Hence, once the input voltage drops below this limit, no power will be supplied to the load by the supercapacitor. This result has proven the working of the proposed

**Table 2**
**Experimental and Simulation results**

| | *Simulation* | *Experimental* | *Units* |
|---|---|---|---|
| Freq. | 1 | 1 | MHz |
| Duty cycle | 50 | 50 | % |
| $Pi_n$ | 240 | 240 | mW |
| $P_{out}$ | 105 | 98 | mW |
| $V_{out}$ | 3.30 | 3 | V |
| $G_{link}$ | 43.8 | 39.89 | % |

hybrid energy storage system. However, it should be recognized that the specific voltage threshold level may need to be adjusted to suit the device used, and meet the manufactures recommendations. For example, a lower threshold voltage of 2.5 V and upper threshold voltage of 5.3 V may be more suitable for improving long-term reliability for the supercapacitor.

## 5. CONCLUSION

A wireless power supply with hybrid super capacitor and battery storage has been developed for powering implantable devices, such as ICP monitors. The primary circuit includes a class E self-oscillator for magnetic field generation and the secondary power pickup consists of a resonant tuning circuit and a current doubler rectifier for charging the super capacitor and the battery. The results show that the measured efficiency of 49.6% is achieved by the system, which is 21% increase as compared to the existing method.

## REFERENCES


[1] E. Stehlin, S. Malpas, P. Heppner, P. Hu, M. Lim and D. Budgett, *Intracranial Pressure and Brain Monitoring XIV*, vol. 114, pp. 101-104, 2012, Springer Verlag.

[2] M. Porter, “Reliability considerations for implantable medical ICs”, *Proc. IEEE Int. Rel. Phys. Symp. (IRPS)*, pp. 516-523.

[3] H. Y. Leung, D. M. Budgett and A. P. Hu, “Minimizing power loss in air-cored coils for TET heart pump systems”, *IEEE J. Emerg. Sel. Topics Circuits Syst.*, vol. 1, no. 3, pp. 412-419, 2011.

[4] T. Dissanayake, D. Budgett, A. P. Hu, S. Malpas and L. Bennet, “Transcutaneous energy transfer system for powering implantable biomedical devices”, *Proc. 13th Int. Conf. Biomed. Eng.*, vol. 23, pp. 235-239.

[5] W. Li and G. Joós, “A power electronic interface for a battery supercapacitor hybrid energy storage system for wind applications”, *Proc. IEEE Power Electron. Specialists Conf. (PESC)*, pp. 1762-1768.

[6] D. Shin, Y. Kim, J. Seo, N. Chang, Y. Wang and M. Pedram, “Battery-supercapacitor hybrid system for high-rate pulsed load applications”, *Proc. Design, Autom. Test Europe Conf. Exhibit. (DATE)*, pp. 1-4.

[7] Mirhoseini and F. Koushanfar, “HypoEnergy. Hybrid supercapacitor-battery power-supply optimization for energy efficiency”, *Proc. Design, Autom. Test Eur. Conf. Exhibit. (DATE)*, pp. 1-4.

[8] U.-M. Jow and M. Ghovanloo, “Design and optimization of printed spiral coils for efficient transcutaneous inductive power transmission”, *IEEE Trans. Biomed. Circuits Syst.*, vol. 1, no. 3, pp. 193-202, 2007.

[9] M. Zierhofer and E. S. Hochmair, “Coil design for improved power transfer efficiency in inductive links”, *Proc. 18th Annu. Int. Conf. IEEE Eng. Med. Biol. Soc., Bridging Disciplines Biomed.*, vol. 4, pp. 1538-1539.

[10] P. Hu, I. L. W. Kwan, C. Tan and Y. Li, “A wireless battery-less computer mouse with super capacitor energy buffer”, *Proc. 2nd IEEE Conf. Ind. Electron. Appl. (ICIEA)*, pp. 2024-2029.

[11] M. Ghovanloo and S. Atluri, “A wide-band power-efficient inductive wireless link for implantable microelectronic devices using multiple carriers”, *IEEE Trans. Circuits Syst. I, Reg. Papers*, vol. 54, no. 10, pp. 2211-2221, 2007.

[12] M. Zierhofer and E. S. Hochmair, “High-efficiency coupling-insensitive transcutaneous power and data transmission via an inductive link”, *IEEE Trans. Biomed. Eng.*, vol. 37, no. 7, pp. 716-722, 1990.

[13] P. Hu, “Selected resonant converters for IPT power supplies”, 2001.

[14] Wang, A. P. Hu and D. M. Budgett, “Development of a push-pull current doubler synchronous rectifier for powering heart pumps”, *Proc. 5th IEEE Conf. Ind. Electron. Appl. (ICIEA)*, pp. 1368-1372.

[15] K. Chen and Z. Zhao, “Analysis of the double-layer printed spiral coil for wireless power transfer”,*IEEE J. Emerg. Sel. Topics Power Electron.*, vol. 1, no. 2, pp. 114-121, 2013.